Noncovalent Bicomponent Self-Assemblies on a Silicon Surface

Bulent Baris,[†] Judicaël Jeannoutot,[†] Vincent Luzet,[†] Frank Palmino,[†] Alain Rochefort,[‡] and Frédéric Chérioux[†,*]

[†]Institut FEMTO-ST, Université de Franche-Comté, CNRS, ENSMM, 32, Avenue de l'Observatoire, F-25044 Besançon Cedex, France and [‡]Département de génie physique and Regroupement québécois sur les matériaux de pointe (RQMP), École Polytechnique de Montréal, CP 6079, Succ. Centre-ville, Montréal, Canada H3C 3A7

ABSTRACT Two-dimensional supramolecular multicomponent networks on surfaces are of major interest for the building of highly ordered functional materials with nanometer-sized features especially designed for applications in nanoelectronics, energy storage, sensors, *etc.* If such molecular edifices have been previously built on noble metals or HOPG surfaces, we have successfully realized a 2D open supramolecular framework on a silicon adatom-based surface under ultrahigh vacuum with thermal stability up to 400 K by combining molecule–molecule and molecule–silicon substrate interactions. One of these robust open networks was further used to control both the growth and the periodicity of the first bicomponent arrays without forming any covalent bond with a silicon surface. Our strategy allows the formation of a well-controlled long-range periodic array of single fullerenes by site-specificity inclusion into a bicomponent supramolecular network.

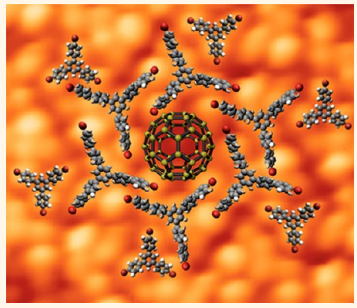

KEYWORDS: supramolecular self-assembly · scanning probe microscopy · semiconductors · surface chemistry · bicomponent network

The fabrication of ordered nanostructure arrays over macroscopic areas, with thermal stability at least at room temperature, would constitute a breakthrough for molecular nanodevice applications.[1−3] Moreover, in order to preserve the pristine unique properties of the targeted molecules in the nanostructures, the cohesion of networks requires selective and noncovalent interactions. To achieve functional nanostructures, multicomponent supramolecular assemblies on noble metal surfaces or HOPG surfaces have been widely investigated.[4−20] However, this type of heteromolecular noncovalent architecture has never been observed on a silicon adatom-based surface. Indeed, for heteromolecular networks, the interactions involved in the building up of the networks are more complex due to combination of molecule–molecule and molecule–substrate interactions. In contrast to noble metal or HOPG surfaces, this complex problem is exacerbated in the case of semiconductive surfaces where molecule–substrate interactions cannot be neglected with respect to molecule–molecule interactions. These strong molecule–substrate interactions can be helpful for nanostructuration by covalent grafting, but their presence can also dramatically disrupt the growth of a supramolecular edifice.[21,22] Successful attempts that avoid strong molecule–substrate interactions on semiconductors have been rarely observed.[23−29] Nevertheless, the use of inexpensive semiconductive substrates[30] still constitutes a prerogative in the development of many devices, such as for molecular electronics, energy conversion, *etc.*

In the present paper, we describe the creation of the first large-scale engineered open heteromolecular supramolecular framework on a silicon adatom surface in the absence of covalent bonds between molecules and substrate. This was achieved by using a Si(111)-B $\sqrt{3} \times \sqrt{3}$R30° reconstructed surface and specifically designed molecular building blocks. The nanostructures were investigated by ultrahigh vacuum scanning tunneling microscopy (UHV-STM), DFT calculations, and STM image simulations. These networks were further used as the template for the growth of a periodic noncompact fullerene array with a thermal stability up to 300 K.

RESULTS AND DISCUSSION

The Si(111)-B $\sqrt{3} \times \sqrt{3}$R30° surface, obtained by specific ultrahigh vacuum (UHV) thermal treatment of commercially available wafers, possesses the unique characteristic of showing depopulated dangling bonds due to the presence of boron atoms located underneath the top silicon layer.[25−27] Therefore, molecule–substrate interactions are weak enough for molecules to diffuse on the surface and strong enough for controlling the growth of the supramolecular network through a surface template effect.

* Address correspondence to frederic.cherioux@femto-st.fr.

Received for review April 26, 2012 and accepted June 30, 2012.

Published online June 30, 2012
10.1021/nn301827e

The distance between two silicon atoms on this surface is 0.66 nm. This value is also close to the distance between the centers of phenyl rings involved in a 1,3,5-triphenylbenzene core (see Figure 1). This distance matching has been recently used for the formation of a commensurable large-scaled 2D open supramolecular network of 1,3,5-tri(4′-bromophenyl)benzene (TBB, Figure 1a) on the Si(111)-B surface.[29] For the present work, we have chosen the 1,3,5-tri(4″-bromo-4,4′-biphenyl)benzene molecule (BPB, Figure 1b) that is built around a 1,3,5-triphenyl core. BPB possesses an additional phenyl ring on each arm that allows us to investigate the possibility of extending the size of the nanopores and their periodicity in the network.

Figure 2a shows a typical large-scale STM image, obtained in the 100−300 K temperature range, of the BPB/Si(111)-B interface around submonolayer molecule coverage. Resolution of STM images acquired at 100 K is similar to those obtained at room temperature (see Figure S1 in Supporting Information). The network is stable up to 400 K (see Figure S2 in Supporting Information). No isolated molecule was observed on a free Si(111)-B surface. The adsorption of BPB on Si(111)-B leads to the formation of a monolayer (Figure S3 in Supporting Information). Monolayer is constituted by a 2D nanoporous network showing three-fold symmetry wherein protrusions have a different brightness from each other. The distance between two disjoined protrusions is 0.65 nm. The nanoporous network is based on hexagonal nanopores (side: 1.1 nm) surrounded by

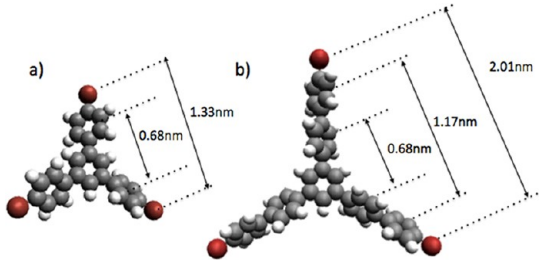

Figure 1. CPK (Corey−Pauling−Koltum) model of (a) 1,3,5-tri(4′-bromophenyl)benzene (TBB) and (b) 1,3,5-tri(4″-bromo-4,4′-biphenyl)benzene (BPB).

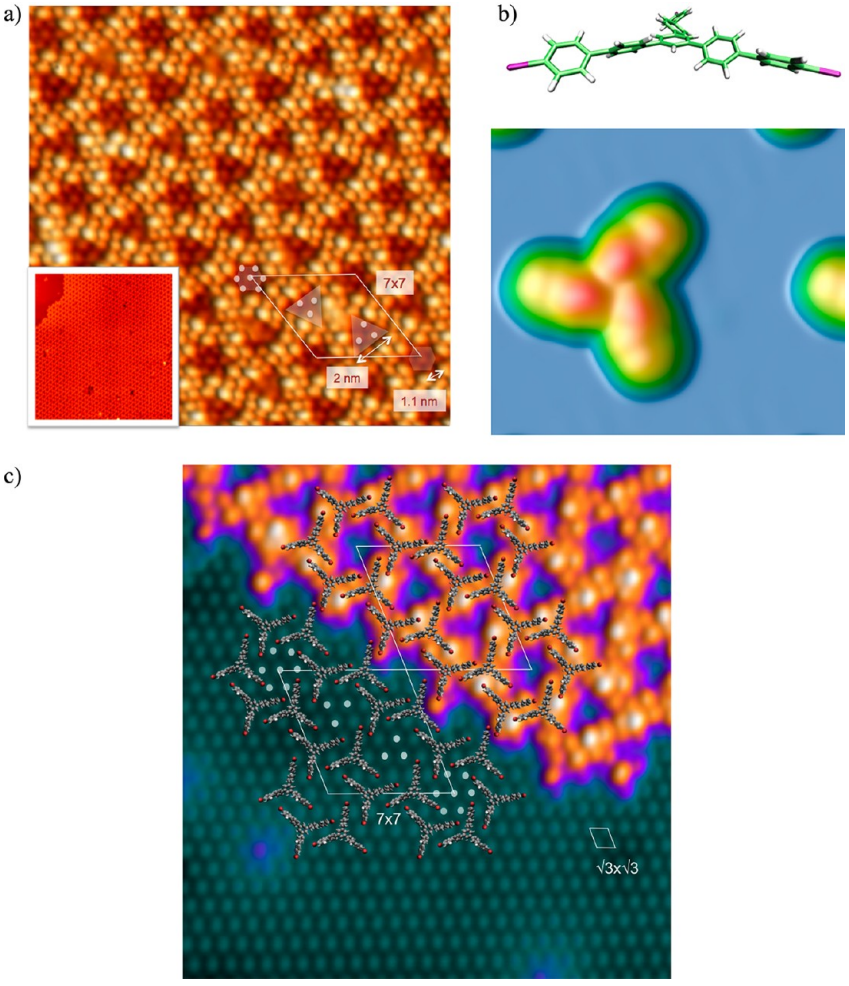

Figure 2. (a) STM image of BPB deposited on the Si(111)-B surface (20 × 20 nm^2, V_s = 2.0 V, I_t = 0.015 nA, 100 K), with a large-scale STM image as an inset (90 × 100 nm^2, V_s = 2.0 V, I_t = 0.02 nA, 100 K). (b) Simulated STM image of an adsorbed BPB molecule with a geometry similar to the given model (top) obtained in a constant current mode (V_s = 2.0 V, I_t = 0.01 nA). (c) Superimposed model of BPB network on both the Si(111)-B surface and molecular network.

six triangular nanopores (side: 2.0 nm), oriented at 60° from one to the other. Seven protrusions are observed within a hexagonal nanopore, while for a triangular nanopore, only three protrusions (white dots in Figure 2) can be seen. The periodicity of the network is 7 × 7, and the network forms a commensurable structure with the $\sqrt{3} \times \sqrt{3}$ reconstruction of the Si(111)-B surface (Figure 2).

Given the dimensions of BPB molecules, six disjoined protrusions are attributed to one BPB molecule and two protrusions correspond to a BPB arm. This hypothesis is strongly supported by STM image simulation. Figure 2b shows the simulated STM image of an isolated BPB molecule (top of Figure 2b) with multiple protusions where the main contrasts correspond to the individual tilted phenyl groups attached to the central ring. In agreement with our DFT results (DFT/B3LYP+D,6-31G*) for an isolated BPB molecule and a dimer, we do not clearly distinguish the contrast associated with terminal Br atoms in the simulated STM image since the major conducting states of this species that would contribute to the calculated STM signal are located around 10 eV above Fermi energy. Then, the different contrasts associated with bromine that are observed experimentally have to be strongly dependent on where the Br atom is sitting on the Si(111)-B surface; we may expect high contrast where the density of states of surface atoms is large. In addition, as shown in the Supporting Information (see Figure S4), a 33° rotation of any phenyl group in isolated BPB necessitates less than 2.5 kcal/mol, and some of these phenyl groups are even nearly free to rotate. Since the interaction energy between BPB molecules is more significant than energy for phenyl rotation and the surface corrugation should also influence the adsorbate structure, the geometry of adsorbed BPB and its associated STM image (see Figure S5 in Supporting Information) can be drastically different from the gas phase structure. As a result, the geometry of BPB used in the STM simulation corresponds to the gas phase geometry but where we have considered a rigid rotation of terminal bromophenyl by 33° with respect to the more central benzene ring. Although the evaluation of an exact rotation angle of phenyl groups on the Si(111)-B surface would necessitate extensive calculations on a large unit cell, the rigid rotation considered here allows us to reproduce the main features of experimental STM results.

From the high-resolution STM image observed near the step edge island, and supported by our simulated STM images, the proposed molecular network adsorbed on the Si(111)-B surface schematized in Figure 2c is fully consistent with an ordered commensurate BPB adlayer. The adsorption of BPB can be described by the position of one bromophenyl group and one Br atom from one of the two remaining arms, respectively, located between three Si adatoms (see green circles in Figure 3) and above a Si adatom (see yellow circles in Figure 3). Overall molecular

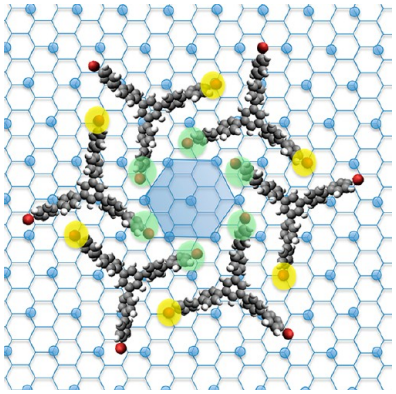

Figure 3. Position of Br atoms above silicon adatoms (yellow circles) and between silicon adatoms (green circles) of the BPB molecule on a Si(111)-B surface.

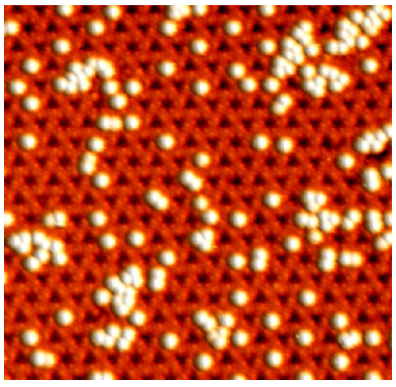

Figure 4. STM images of C_{60} onto the BPB supramolecular network deposited on the Si(111)-B surface (60 × 60 nm^2, V_s = 2.2 V, I_t = 0.15 nA, 110 K). C_{60} molecules are adsorbed in hexagonal nanopores, in triangular nanopores, or onto the BPB network.

arrangement and the BPB molecular dimension explain the formation of the two types of nanopores. The darker protrusions located in each nanopore (dots in Figure 2c) are attributed to Si adatoms of the uncovered $\sqrt{3} \times \sqrt{3}$ reconstruction. According to this proposed network, one can clearly see that the highest constrast is always associated with the terminal Br atoms sitting on a surface Si adatom where the density of states (DOS) is higher than that for the two other sites where the remaining Br atoms are located. Hence, the magnitude of contrast observed for any Br atom is directly related to its adsorption site; the highest are observed for the Br atom in the vicinity of a surface Si adatom.

Since no isolated molecule is observed in the 100−400 K range, we may conclude that BPB molecules diffuse easily on the Si(111)-B surface in order to form the self-assembly. In this supramolecular network, the stabilization of molecule−molecule interactions should arise mostly from $\pi-\pi$ attractions between tilted phenyl rings (Figure 2c).[31] This statement is supported by DFT calculations on two different dimers (see Figure S6 in Supporting Information) in which the presence of a Br atom improves the stability of the complex only by 5%. Although the

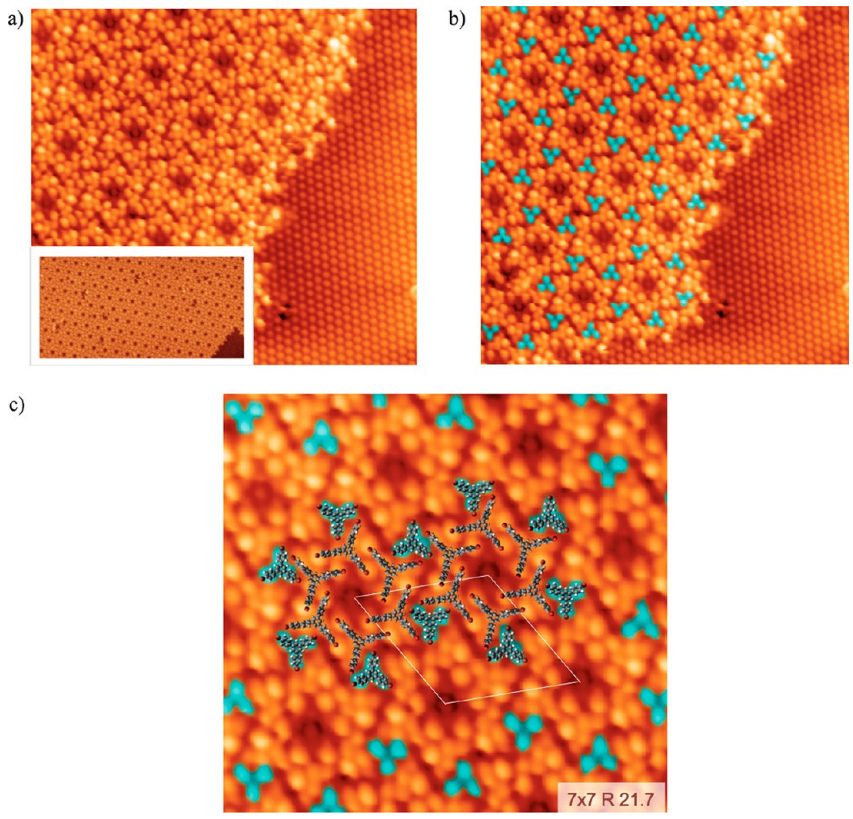

Figure 5. (a) STM images of TBB onto the BPB supramolecular network on Si(111)-B surface (34 × 34 nm^2, V_s = 2.0 V, I_t = 0.02 nA, 100 K) with a large-scale STM image as an inset (99 × 55 nm^2, V_s = 2.0 V, I_t = 0.02 nA, 100 K). (b) Same STM image shown in (a) with triangle filling highlighted in blue. (c) Superimposed model of the TBB/BPB network on the Si(111)-B surface.

exact nature of such $\pi-\pi$ interactions is still not totally clear, a mechanism involving a sort of dipole−dipole interaction such as in CH$-\pi$ is often discussed.[32,33] Given the chemical nature of BPB, a stabilization of the assembly by such CH$-\pi$ interactions (including CBr$-\pi$) is quite realistic. Nevertheless, molecule−substrate interaction appears strong enough in the self-assembly to direct BPB molecules onto in a single type of adsorption site (Si adatom) where one over three Br atoms is sitting and that forces the formation of an open network instead of a compact self-assembly (see Figure 2c and Figure S7 in Supporting Information). Therefore, thermal stability of the BPB network above room temperature is justified by molecule−molecule and molecule−substrate attractive interactions.

Trapping of fullerenes in molecular nanoporous networks on surfaces was widely investigated to promote the formation of a periodic C_{60} array.[12−19] In our case, the filling of each BPB nanopore by a single C_{60} molecule was considered because the size of all nanopores (1.1 nm) and covalent diameter of C_{60} (0.8 nm) are nicely matching.

Figure 4 shows an STM image, recorded at 110 K, of C_{60} molecules adsorbed onto nanopores of a BPB molecular network. The measured diameter of these very bright protrusions (2 nm) is compatible with the van der Waals diameter of C_{60} observed with STM by other groups.[12] Therefore, each protrusion is attributed to a single C_{60} molecule adsorbed above the nanoporous BPB network. No clear fullerene organization is observed onto the BPB network: 66% of C_{60} molecules are adsorbed onto BPB network as small clusters. For isolated C_{60} molecules, 6% are adsorbed in triangular nanopores and 28% are adsorbed in hexagonal nanopores (Figure 4).

In order to form a high-level periodic array of fullerene molecules onto the BPB network, we need to find a strategy for compelling a more specific C_{60} adsorption in hexagonal nanopores of the BPB network. This could be achieved by avoiding any adsorption in triangular nanopores of the BPB network. Triangular nanopores have 2.0 nm sides (Figure 2a), which is strongly consistent with dimension of TBB molecules (see Figure 1b). This size matching could be beneficial for the specific adsorption of TBB in triangular nanopores of the BPB network. Therefore, TBB molecules were deposited onto BPB network. STM Images are described in Figure 5a−c.

Large-scale STM images of the TBB/BPB/Si(111)-B interface have been obtained at 100 K (Figure 5a,b) and at 300 K (Figure S8 in in Supporting Information). No TBB molecule is observed on the free Si(111)-B surface. Monolayers are constituted by a 2D nanoporous network showing a three-fold symmetry. By comparison with STM images of the BPB network (Figure 2a), only hexagonal nanopores (side: 1.1 nm) are now observed,

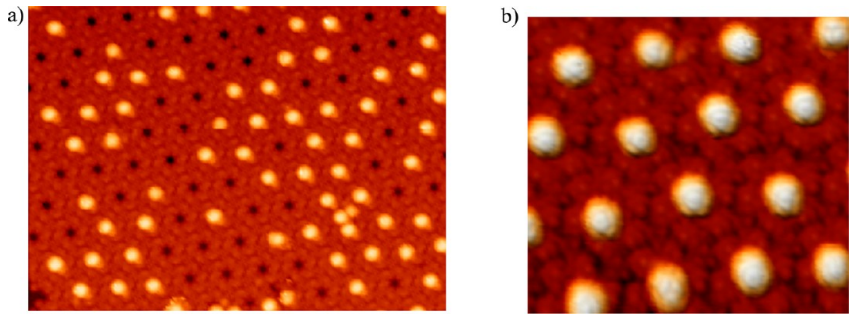

Figure 6. (a) STM images of C_{60} adsorbed on the TBB/BPB network on the Si(111)-B surface (36 × 50 nm^2, V_s = 2.2 V, I_t = 0.01 nA, room temperature). (b) STM image showing electronic substructure of C_{60} and TBB onto the BPB network on the Si(111)-B surface (20 × 17 nm^2, V_s = 2.4 V, I_t = 0.01 nA, 100 K).

and the entire amount of triangular nanopores has disappeared. All triangular nanopores previously observed in the BPB network are now filled by three disjoined protrusions. These three protrusions are consistent with STM images recorded for the TBB network on the Si(111)-B surface.[29] Therefore, these protrusions are attributed to adsorbed TBB molecules in triangular nanopores of the BPB network. The periodicity of the network is still 7 × 7 but is rotated by 21.7° and is always commensurable with the $\sqrt{3} \times \sqrt{3}$ reconstruction of the Si(111)-B surface (Figure 5a).

On the basis of STM images, a superimposed model for the TBB/BPB/Si(111)-B interface is described in Figure 5c. As expected, no TBB molecules are adsorbed into hexagonal nanopores. This result is consistent with the adsorption site of TBB on Si(111)-B that is only existing in triangular nanopores,[29] leading to a specific adsorption of TBB onto the BPB network. We anticipate that TBB−BPB interactions are related to $\pi-\pi$ interactions between a tilted phenyl group of TBB molecules and biphenyl arms of BPB molecules. The 21.7° rotation of TBB/BPB/Si(111)-B relative to BPB/Si(111)-B accentuates the TBB−BPB $\pi-\pi$ interactions (see Figure S9 in Supporting Information). All of these attractive interactions ensure thermal stability of the supramolecular network.

As the TBB/BPB supramolecular network exhibits only a single type of nanopores, with sides equal to 1.1 nm, C_{60} molecules were deposited onto this interface. A periodic array of bright protrusions onto the TBB/BPB/Si(111)-B network is observed in STM images (Figure 6). Less than 5% of C_{60} molecules appear as a small cluster. These bright protrusions (2 nm of diameter) are exactly located on hexagonal nanopores of the TBB/BPB network. Therefore, these protrusions are attributed to a single fullerene molecule sitting on a hexagonal nanopore of the TBB/BPB network.

The periodicity of C_{60}/TBB/BPB/Si(111)-B network is still 7 × 7 and is always commensurable with the $\sqrt{3} \times \sqrt{3}$ reconstruction of the Si(111)-B surface (Figure 6b and Figure S10 in Supporting Information). This network is stable up to 300 K (see Figure S11 in Supporting Information). The periodic self-assembly is based on specific adsorption of TBB molecules on the BPB network and specific adsorption of C_{60} onto the TBB/BPB network. Therefore, intermolecular distance between C_{60} is 4.65 nm. In such bicomponent self-assembly, the geometrical design of C_{60} patterns is of primary interest for heterojunction solar cells, in order to ensure the commensurability of exciton dissociation interfacial area and the exciton diffusion length (5−10 nm).[34]

CONCLUSIONS

We report the formation of a bicomponent supramolecular network on a silicon surface with a thermal stability up to 300 K. This framework has been achieved by exploiting the interactions between molecules and substrate. By tuning the size of molecules built from a 1,3,5-triphenyl core, well-defined supramolecular networks have been obtained with a controlled long distance (4.6 nm) between nanopores. This approach opens the route toward a new class of robust and commensurable organic networks on a silicon substrate.

METHODS

Molecule and Substrate Preparation. 1,3,5-Tri(4′-bromophenyl)-benzene was purchased from Aldrich and then purified by column chromatography on silica gel and then sublimated. C_{60} was purchased from Aldrich and used without further purification. 1,3,5-Tri(4″-bromo-4,4′-biphenyl)benzene was synthetized by cyclotrimerization of 4′-bromophenyl-4-acetophenone.[35−37] Molecules were then purified by column chromatography on silica gel and sublimated.

The Si(111)-B $\sqrt{3} \times \sqrt{3}$R30° reconstruction surface is prepared by annealing of the (111) surface of a highly B-doped Si wafer (0.001 W·cm resistivity). Si(111) surface is carefully outgassed and cleaned *in situ* by a series of rapid heating up to 1200 °C under a pressure lower than 5×10^{-10} mbar. A thermal process (1 h at 800 °C) activates the boron segregation at the surface, and a maximum boron atom concentration of 1/3 monolayer (ML) can be obtained (one ML is referred to the Si(111) ideal surface atomic density with 7.8×10^{14} atoms·cm^{-2}). In these conditions, the surface exhibits a perfect $\sqrt{3} \times \sqrt{3}$R30° reconstruction.

STM Experiments. STM experiments were performed in an ultrahigh vacuum chamber with a base pressure lower than 2×10^{-10} mbar equipped with a variable temperature Omicron scanning tunneling microscope (STM). STM images were

acquired in a constant-current mode at room temperature or 100 K. 1,3,5-Tri(4′-bromophenyl)benzene (TBB) and C_{60} molecules were deposited from a quartz crucible at 160 and 350 °C, respectively. The Si(111)-B substrate was kept at room temperature during the sublimation. Each image process was carried out using WSXM software.[38]

STM Image Simulation. STM simulations were carried out with the SPAGS-STM software,[39] in which we used an electron scattering approach included in our parallel Landauer−Buttiker solver in conjunction with a tight-binding Hamiltonian that reproduces DFT results. DFT calculations on isolated species were performed with the NwChem software[40] where we used the B3LYP functional (6-31G*) and the semiempirical approach of Grimme to evaluate the contribution of dispersion and van der Waals interaction to the DFT energy.[41]

Prior to any STM simulations, DFT calculations were performed on an isolated BPB molecule to obtain the optimized geometry. Since the size of a single unit cell representing the multicomponent system is computationally prohibitive, in addition to the fact that the adsorbed molecules are weakly interacting with the substrate, we have limited our STM simulation to a single BPB molecule physisorbed on a Cu(111) surface. In this manner, we exclude a contribution from the substrate to the STM contrast. In the STM simulations, we have studied the influence of the rotation of the terminal bromophenyl groups on the resulting STM images. We found that a rotation of +33° of terminal groups (the middle phenyl groups are rotated by −33°) that were originally flat with respect to the central benzene ring gives a good agreement with experimental STM images. On the basis of our DFT calculations, a single phenyl rotation of 33° would need less than 2.5 kcal/mol to occur for a fully relaxed structure.

Conflict of Interest: The authors declare no competing financial interest.

Acknowledgment. This work is supported by the Pays de Montbéliard Agglomération, the région de Franche-Comté, and the French Agency ANR (ANR-09-NANO-038). A.R. is grateful to Calcul Québec and Calcul Canada for providing computational resources.

Supporting Information Available: Additional figures. This material is available free of charge *via* the Internet at http://pubs.acs.org.

REFERENCES AND NOTES

1. Joachim, C.; Gimzewski, J.; Aviram, A. Electronics Using Hybrid-Molecular and Mono-Molecular Devices. *Nature* **2000**, *408*, 541–548.
2. Barth, J. V.; Constantini, G.; Kern, K. Engineering Atomic and Molecular Nanostructures at Surfaces. *Nature* **2005**, *437*, 671–679.
3. Bartels, L. Tailoring Molecular Layers at Metal Surfaces. *Nat. Chem.* **2010**, *2*, 87–95.
4. Canas-Ventura, M. E.; Aït-Mansour, K.; Ruffieux, P.; Rieger, R.; Müllen, K.; Brune, H.; Fasel, R. Complex Interplay and Hierarchy of Interactions in Two-Dimensional Supramolecular Assemblies. *ACS Nano* **2011**, *5*, 457–469.
5. Elemans, J. A. A. W.; Lei, S.; De Feyter, S. Molecular and Supramolecular Networks on Surfaces: From Two-Dimensional Crystal Engineering to Reactivity. *Angew. Chem., Int. Ed.* **2009**, *48*, 7298–7333.
6. Shi, Z.; Lin, N. Structural and Chemical Control in Assembly of Multicomponent Metal-Organic Coordination Networks on a Surface. *J. Am. Chem. Soc.* **2010**, *132*, 10756–10761.
7. Xiao, W.; Passerone, D.; Ruffieux, P.; Aït-Mansour, K.; Gröning, O.; Tosatti, E.; Siegel, J. S.; Fasel, R. C_{60}/Corannulene on Cu(110): A Surface-Supported Bistable Buckybowl−Buckyball Host−Guest System. *J. Am. Chem. Soc.* **2008**, *130*, 4767–4771.
8. Huang, Y. L.; Chen, W.; Wee, A. T. S. Molecular Trapping on Two-Dimensional Binary Supramolecular Networks. *J. Am. Chem. Soc.* **2011**, *133*, 820–825.
9. Calmettes, B.; Nagarajan, S.; Gourdon, A.; Abel, M.; Porte, L.; Coratger, R. Bicomponent Supramolecular Packing in Flexible Phthalocyanine Networks. *Angew. Chem., Int. Ed.* **2008**, *47*, 6994–6998.
10. Yoshimoto, S.; Honda, Y.; Ito, O.; Itaya, K. Supramolecular Pattern of Fullerene on 2D Bimolecular "Chessboard" Consisting of Bottom-Up Assembly of Porphyrin and Phtalocyanine Molecules. *J. Am. Chem. Soc.* **2008**, *130*, 1085–1092.
11. Blunt, M. O.; Russell, J. C.; Gimenez-Lopez, M. C.; Taleb, N.; Lin, X.; Schröder, M.; Champness, N. R.; Beton, P. H. Guest-Induced Growth of a Surface-Based Supramolecular Bilayer. *Nat. Chem.* **2011**, *3*, 74–78.
12. Moriarty, P. J. Fullerene Adsorption on Semiconductor Surfaces. *Surf. Sci. Rep.* **2010**, *65*, 175–227.
13. Piot, L.; Silly, F.; Tortech, L.; Nicolas, Y.; Blanchard, P.; Roncali, J.; Fichou, D. Long-Range Alignments of Single Fullerenes by Site-Selective Inclusion into a Double-Cavity 2D Open Network. *J. Am. Chem. Soc.* **2009**, *131*, 12864–12865.
14. Theobald, J. A.; Oxtoby, N. S.; Champness, N. R.; Beton, P. H.; Dennis, T. J. S. Growth Induced Reordering of Fullerene Clusters Trapped in a Two-Dimensional Supramolecular Network. *Langmuir* **2005**, *21*, 2038–2041.
15. Theobald, J. A.; Oxtoby, N. S.; Philipps, M. A.; Champness, N. R.; Beton, P. H. Controlling Molecular Deposition and Layer Structure with Supramolecular Surface Assemblies. *Nature* **2003**, *424*, 1029–1031.
16. Macloed, J. M.; Ivasenko, O.; Fu, C.; Taerum, T.; Roseï, F.; Perepichka, D. Supramolecular Ordering in Oligothiophene-Fullerene Monolayers. *J. Am. Chem. Soc.* **2009**, *131*, 16844–16850.
17. Bonifazi, D.; Kiebele, A.; Stohr, M.; Cheng, F.; Jung, T.; Diederich, F.; Spillmann, H. Supramolecular Nanostructuring of Silver Surfaces *via* Self-Assembly of [60]Fullerene and Porphyrin Modules. *Adv. Funct. Mater.* **2007**, *17*, 1051–1062.
18. Mena-Osteritz, E.; Bäuerle, P. Complexation of C_{60} on a Cyclothiophene Monolayer Template. *Adv. Mater.* **2006**, *18*, 447–451.
19. Stepanow, S.; Lingenfelder, M.; Dmitriev, A.; Spillmann, H.; Delvigne, E.; Lin, N.; Deng, X.; Cai, C.; Barth, J. V.; Kern, K. Steering Molecular Organization and Host−Guest Interactions Using Two-Dimensional Nanoporous Coordination Systems. *Nat. Mater.* **2004**, *3*, 229–233.
20. Ruben, M.; Payer, D.; Landa, A.; Comisso, A.; Gattinoni, C.; Lin, N.; Collin, J.-P.; Sauvage, J.-P.; De Vita, A.; Kern, K. 2D Supramolecular Assemblies of Benzene-1,3,5-triyl-tribenzoic Acid: Temperature-Induced Phase Transformations and Hierarchical Organization with Macrocyclic Molecules. *J. Am. Chem. Soc.* **2006**, *128*, 15644–15651.
21. (a) Hossain, M. Z.; Kato, H. S.; Kawai, M. Self-Directed Chain Reaction by Small Ketones with the Dangling Bond Site on the Si(100)-(2 × 1)-H Surface: Acetophenone, a Unique Example. *J. Am. Chem. Soc.* **2008**, *130*, 11518–11523. (b) Lopinski, G. P.; Wayner, D. D. M.; Wolkow, R. A. Self-Directed Growth of Molecular Nanostructures on Silicon. *Nature* **2000**, *406*, 48–51.
22. Harikumar, K. R.; Leung, L.; McNab, I. R.; Polanyi, J.-C.; Lin, H. P.; Hofer, W. A. Cooperative Molecular Dynamics in Surface Reactions. *Nat. Chem.* **2009**, *1*, 712–716.
23. Hamers, R.; Coulter, S. K.; Ellison, M. D.; Hovis, J. S.; Padowitz, D. F.; Schwartz, M. P.; Greenlief, C. M.; Russell, J. N. Cycloaddition Chemistry of Organic Molecules with Semiconductor Surfaces. *Acc. Chem. Res.* **2000**, *33*, 617–624.
24. Sloan, P. A.; Palmer, R. E. Two-Electron Dissociation of Single Molecules by Atomic Manipulation at Room Temperature. *Nature* **2005**, *434*, 367–371.
25. Makoudi, Y.; Arab, M.; Palmino, F.; Duverger, E.; Ramseyer, C.; Picaud, F.; Cherioux, F. A Stable Room-Temperature Molecular Assembly of Zwitterionic Organic Dipole Guided by a Si(111)-7 × 7 Template Effect. *Angew. Chem., Int. Ed.* **2007**, *46*, 9287–9290.
26. Lyo, I.-W.; Kaxiras, E.; Avouris, Ph. Adsorption of Boron on Si(111)—Its Effect on Surface Electronic States and Reconstruction. *Phys. Rev. Lett.* **1989**, *62*, 1261–1264.
27. Makoudi, Y.; Palmino, F.; Duverger, E.; Arab, M.; Cherioux, F.; Ramseyer, C.; Therrien, B.; Tschan, M. J.-L.; Süss-Fink, G.

Non-destructive Room-Temperature Adsorption of 2,4,6-Tri(2′-thienyl)-1,3,5-triazine on a Si-B Interface: High-Resolution STM Imaging and Molecular Modeling. *Phys. Rev. Lett.* **2008**, *100*, 076405.
28. Makoudi, Y.; Arab, M.; Palmino, F.; Duverger, E.; Cherioux, F. A Complete Supramolecular Self-Assembled Adlayer on a Silicon Surface at Room-Temperature. *J. Am. Chem. Soc.* **2008**, *130*, 6670–6671.
29. Baris, B.; Luzet, V.; Duverger, E.; Sonnet, Ph.; Palmino, F.; Cherioux, F. Robust and Open Tailored Supramolecular Networks Controlled by the Template Effect of a Silicon Surface. *Angew. Chem., Int. Ed.* **2011**, *50*, 4094–4098.
30. A Au(111) single crystal costs $1200, and a piece of silicon wafer costs $0.01.
31. Grimme, S. Do Special Noncovalent $\pi-\pi$ Stacking Interactions Really Exist? *Angew Chem., Int. Ed.* **2008**, *47*, 3430–3434.
32. Rochefort, A.; Wuest, J. D. Interaction of Substituted Aromatic Compounds with Graphene. *Langmuir* **2009**, *25*, 210–215.
33. Gagnon, E.; Rochefort, A.; Métivaud, V.; Wuest, J. D. Hexaphenylbenzenes as Potential Acetylene Sponges. *Org. Lett.* **2010**, *12*, 380–383.
34. Thompson, B. C.; Fréchet, J.-M. J. Polymer-Fullerene Composite Solar Cells. *Angew. Chem., Int. Ed.* **2008**, *47*, 58–77.
35. Lu, J.; Tao, Y.; D'iorio, M.; Li, Y.; Ding, J.; Day, M. Pure Deep Blue Light-Emitting Diodes from Alternating Fluorene/Carbazole Copolymers by Using Suitable Hole-Blocking Materials. *Macromolecules* **2004**, *37*, 2442–2449.
36. Cherioux, F.; Guyard, L.; Audebert, P. Synthesis and Electrochemical Properties of New Star-Shaped Thiophene Oligomers and Their Polymers. *Chem. Commun.* **1998**, 2225–2226.
37. Cherioux, F.; Guyard, L. Synthesis, Molecular Computations and Electrochemical Properties of Original 1,3,5-Tris-(oligothienyl)benzenes Derivatives: A New Generation of 2D or 3D Reticulating Agent. *Adv. Funct. Mater.* **2001**, *11*, 305–309.
38. Horcas, I.; Fernandez, R.; Gomez-Rodriguez, J. M.; Colchero, J.; Gomez-Herrero, J.; Baro, A. M. WsXM: A Software for Scanning Probe Microscopy and a Tool for Nanotechnology. *Rev. Sci. Instrum.* **2007**, *78*, 013705.
39. Janta-Polczynski, B. A.; Cerdá, J. I.; Éthier-Majcher, G.; Piyakis, K.; Rochefort, A. Parallel STM Imaging of Low Dimensional Nanostructures. *J. Appl. Phys.* **2008**, *104*, 023702.
40. Valieva, M.; Bylaskaa, E. J.; Govinda, N.; Kowalskia, K.; Straatsmaa, T. P.; Van Dama, H. J. J.; Wanga, D.; Nieplochaa, J.; Aprab, E.; Windusc, T. L.; *et al.* NWChem: A Comprehensive and Scalable Open-Source Solution for Large Scale Molecular Simulations. *Comput. Phys. Commun.* **2010**, *181*, 1477–1489.
41. Grimme, S. Accurate Description of van der Waals Complexes by Density Functional Theory Including Empirical Corrections. *J. Comput. Chem.* **2004**, *25*, 1463–1473.